The Inversion Wind Pattern over West Antarctica*

THOMAS R. PARISH

Department of Atmospheric Science, University of Wyoming, Laramie, WY 82071

DAVID H. BROMWICH

Institute of Polar Studies, The Ohio State University, Columbus, OH 43210

(Manuscript received 9 November 1984, in final form 13 October 1985)

ABSTRACT

The surface windfield over the gently sloping interior ice fields of Antarctica is characterized by a high degree of persistence in terms of both direction and speed. The forcing of the surface wind is due primarily to the radiational cooling of the air adjacent to the sloping terrain. The representativeness of a simple diagnostic equation system in inferring the surface winds from a knowledge of terrain slope and temperature inversion structure is examined. Results suggest at least qualitatively accurate surface drainage patterns over the Antarctic continent are possible using this technique. A wintertime surface wind simulation for West Antarctica has been generated based on an accurate ice topography map. Close agreement is seen between the simulated surface windfield with field observations and sastrugi orientations. Implications of the simulation are discussed.

1. Introduction

Documentation of the wind and temperature fields over the Antarctic interior (Fig. 1) is extremely sparse. Only a handful of stations have been established in the continental interior during the past thirty years, nearly all of which have since ceased operations. A list of manned meteorological stations in Antarctica with a record of at least two years is given in Schwerdtfeger (1970a). Recently, this data void has been partly eliminated by deployments of automatic weather stations (AWSs) which transmit to polar orbiting satellites (e.g., Bromwich, 1984). Aside from the station records, valuable wind and temperature information is contained within the reports of the numerous traverse expeditions over the continent. In addition, observations by traverse party members of the orientation of sastrugi (aerodynamically-smoothed ridges of snow whose principal axes are parallel to the resultant wind direction) have provided information about prevailing wind directions. From these sources of data, it has been established that the surface windfield over the Antarctic interior is highly persistent both in direction and speed and is closely coupled to the orientation and steepness of the ice terrain.

The strong radiational cooling of air in the lower atmosphere adjacent to the sloping ice terrain is an important component of the energy budget in the near-surface layer and is primarily responsible for the formation and maintenance of the temperature inversion found above the Antarctic ice slopes most of the year. Lettau and Schwerdtfeger (1967) note that a temperature inversion over sloping terrain implies the existence of a horizontal temperature gradient and, consequently, a thermal wind directed parallel to the ice contours with higher ice heights to the right. This sloped-inversion effect is of central importance in understanding the surface wind regime over Antarctica and emphasizes the dominant role played by the ice topography in shaping the near-surface windfield. Parish (1982) has listed directional constancy values for Antarctic interior stations. In general, surface wind directional constancy values range from 0.80 to 0.90 over the entire continent indicating the nearly uni-directional nature of the flow. Unlike the case in midlatitudes, directional constancy values for Antarctic winds are largest near the surface and decrease significantly with height. Schwerdtfeger (1970a) has shown that the directional constancy values at South Pole decrease from a near-surface value of 0.80 to 0.27 about 800 m above ground. Such results clearly indicate the dominant influence of topography in shaping the surface windfield.

A key parameter in understanding the strength and deviation angle of the wind from the fall line is the ice terrain slope. The Antarctic ice fields display a wide spectrum of terrain slopes. Over the high interior plateau, ice terrain slopes are quite gentle with a magnitude of 10^{-3} or less, similar to the slope of the Great Plains in the central United States. Ice slopes are much steeper near the coast, generally reaching 10^{-2} about 100 km from the coast and averaging between 3×10^{-2} to 5

* Contribution 523 of the Institute of Polar Studies, The Ohio State University.

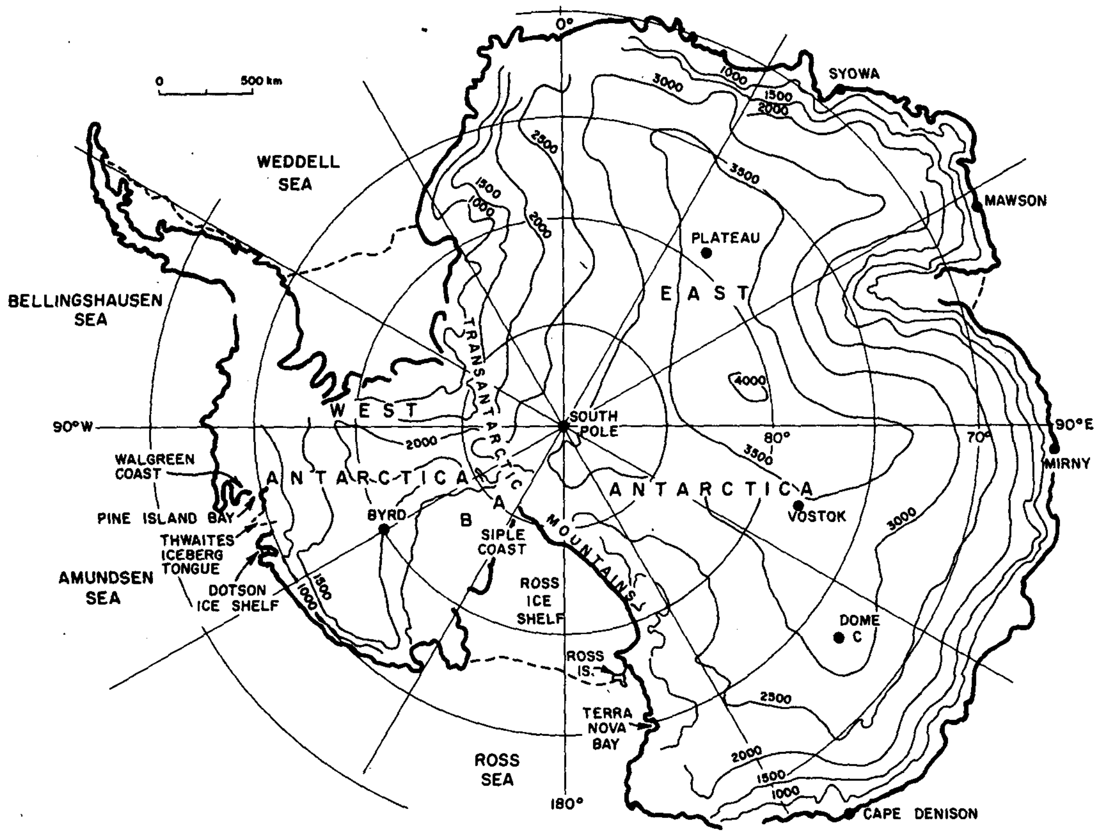

FIG. 1. The Antarctic continent including positions of stations mentioned in text. A and B refer to positions of Ice Stream A and Ice Stream B. Dashed lines indicate seaward edges of ice shelves.

$\times 10^{-2}$ within 10 km of the coast (Mather and Miller, 1966). Due to these dramatic slope variations, drainage flows over the Antarctic interior differ in several respects from near-coastal flows. Schwerdtfeger (1970a) points out that near-surface winds over the Antarctic interior can persist over long time periods, often on the order of weeks. These winds generally are only of moderate strength and show little range in speed. It has been established that these interior winds can be treated as an equilibrium flow with a balance of forces due to pressure gradient, Coriolis and friction. The term "inversion" wind has been used to describe the steady near-surface windfield over the Antarctic interior. Resultant winds at interior stations (see Parish, 1982), presumably dominated by inversion winds, are directed at large angles (50°–60°) from the fall line. As a consequence, inversion winds are inefficient in transporting cold air downslope. This is significant in the maintenance of the inversion windfield since the cold air supply upslope is not readily exhausted as is often the case near steep coastal slopes. The steady-state nature of the inversion windfield implies a balance between cold air production due to radiational cooling and downslope transfer of cold air.

Surface winds over the steep coastal ice slopes of Antarctica differ markedly from inversion winds. Resultant winds from coastal stations show that the flow is significantly stronger than the winds over the continental interior and generally is directed in a more downslope direction in response to stronger terrain-induced accelerations. Some of the strongest winds ever recorded have occurred over the coastal slopes of Antarctica. Schwerdtfeger (1970a) notes that it is only in the near coastal regions where true katabatic winds exist. Unlike inversion winds, katabatic winds are characterized by their nonsteady behavior. Even the most katabatic-prone coastal stations experience periods of near calm followed by sudden blasts of cold air. Streten (1968) concludes that katabatic winds at Mawson station generally persist for periods less than 24 hours except when coupled with cyclonic systems. This behavior is consistent with the cold air supply limitations alluded to above. Even moderate katabatic flow transports a significant amount of negatively-buoyant cold air northward and rapidly exhausts available cold air reserves upslope over the near interior. The strongest katabatic wind regime known is at Cape Denison along the coast of East Antarctica. The anomalous strength and persistence of the wind is a result of the strongly confluent nature of the cold air drainage currents upslope of Cape Denison (Parish, 1981, 1982). Similar katabatic wind conditions downstream of another confluence zone have recently been documented in Terra Nova Bay (Bromwich, 1985). Numerical experiments have shown the katabatic regime to be especially sensitive to the availability of cold air upslope (Parish, 1984).

2. Forcing of surface winds over the Antarctic interior

The dominant forcing mechanism for both inversion and katabatic winds is the radiational cooling of air adjacent to the sloping ice terrain. This results in a horizontal pressure gradient force directed down the fall line. The magnitude of this force is dependent on the terrain slope, inversion strength, and shape and depth of the inversion (see Radok, 1973 and Kodama and Wendler, 1986). The fact that extremely high directional constancy values are recorded at interior stations suggests that the terrain-induced pressure gradient must generally be considerably larger than the synoptic pressure gradient associated with moving cyclonic disturbances. Parish (1982) has shown the relative influence of synoptic systems on the resultant wind over East Antarctica is small. This is in qualitative agreement with results of Schwerdtfeger (1970a) showing weak upper level resultant winds and low directional constancy values at Vostok, South Pole and Byrd stations. Additional confirmation of the relative weakness of synoptic forcing on the time-averaged surface windfield can be found in the record of the AWS installed on the crest of the high ridge known as Dome C. The station operated continuously for three years before failing in January 1983. Because of the nearly flat ice terrain at Dome C (slopes less than 10^{-4}), the sloped-inversion pressure gradient force is very small. Therefore, the surface winds mirror the synoptic forcing. Wendler et al. (1982) note that no relationship is seen between surface temperature and wind speed. The Dome C wind speed and directional constancy are by far the lowest of the interior stations. These facts attest to the relative weakness of upper level forcing on the time-averaged surface wind regime over the Antarctic interior.

Equations of motion for the steady inversion winds over the Antarctic interior in which the fall line is directed along the x-axis can be expressed as follows (Ball, 1960),

$$0 = -g\frac{\Delta T}{\bar{T}}\frac{\partial h}{\partial x} - \alpha\frac{\partial p}{\partial x} + fv - \frac{KVu}{H}, \qquad (1)$$

$$0 = -\alpha\frac{\partial p}{\partial y} - fu - \frac{KVv}{H}, \qquad (2)$$

where ΔT is a measure of the inversion strength, h the ice terrain height, K a frictional constant set at 5×10^{-3} and H the inversion layer depth. Other symbols have their usual meteorological meaning. The first right side term in (1) is the sloped-inversion pressure gradient force; the final terms in both (1) and (2) are drag formulations for the friction term. Assuming a negligible synoptic pressure gradient in the free atmosphere above the inversion layer, Ball (1960) shows the above system can be solved for the inversion wind speed and direction,

$$V = \left(\frac{HF}{K}\right)^{1/2}\cos^{1/2}\beta = -\frac{F}{f}\sin\beta, \qquad (3)$$

$$\beta = \cos^{-1}[(1 + J^2)^{1/2} - J], \qquad (4)$$

where

$$J = \frac{Hf^2}{2KF}, \qquad (5)$$

$$F = -g\frac{\Delta T}{\bar{T}}\frac{\partial h}{\partial x}. \qquad (6)$$

The relationship between surface wind speed and direction with varying ratios of the sloped-inversion pressure gradient force to the synoptic pressure gradient force can be found in Parish (1982). Schwerdtfeger (1970b) notes that the high directional constancy displayed by the surface wind over the Antarctic interior is a result of the dominance of the sloped-inversion effect. Recent work by Cerni and Parish (1984) has shown the inversion quickly reforms after periods of cloudiness and can become fully reestablished within about 24 hours. A rapid recovery of the inversion winds is also necessary to explain the high directional constancy.

Parish (1982) has shown that the above equation system can be used to diagnose time-averaged streamlines of the wintertime surface windfield over East Antarctica with reasonable accuracy. Wind data from interior East Antarctic stations as well as sastrugi orientations (Bromwich and Kurtz, 1984) are in good agreement with the simulation. One limitation to the applicability of (1) and (2) is the assumption that the wind inertia terms are negligible. In Parish (1982), the streamline analysis was terminated near the 2000 m contour to avoid violating this assumption. One way to estimate the magnitude of the inertia term is to solve the preceding equation system over an ice profile corresponding to the near-coastal Antarctic terrain. A revised expression based on the recent ice topography map of Drewry (1983) for the Mirny profile but also representative for much of Antarctica is

$$h = 2780 \text{ m } (r/400 \text{ km})^{0.45}, \qquad (7)$$

where r is the distance in km directed upslope from the coast. The derivative of (7) yields an expression for the slope of the terrain; $(\partial h/\partial r) = (-\partial h/\partial x)$. A series of experiments have been conducted in which the windfield is determined over the idealized ice profile. Various inversion strengths have been assumed in order to cover the range of observed values. The results of wind speeds diagnosed by the equation system are shown in Fig. 2a. Clearly, the wind speeds are directly related to the strength of the terrain-induced pressure gradient. The highest wind speeds are associated with steep slopes and strong inversions. Deviation angles of the wind from the fall line for the wind speeds shown in Fig. 2a are illustrated in Fig. 2b. The wind becomes directed more downslope as the sloped-inversion pressure gradient increases. The smallest deviation angles are, therefore, associated with strongest winds. The model wind characteristics revealed in Figs. 2a and 2b are representative of the observed behavior of the Antarctic surface windfield. A comprehensive review of observed Antarctic surface wind features can be found in Mather and Miller (1967).

One simplification in the above analysis is the assumption of a constant inversion strength over the entire spectrum of terrain slopes. Observations show that the inversion strengths increase from relatively small values near the coast to quite large values over the continental interior. In an attempt to account for these observations, an analysis has been made assuming inversion strengths increase from 2.5°C at the coast to 7°C over the near interior based on the work of Phillpot and Zillman (1970). The dashed lines in Figs. 2a and 2b show resulting wind speeds and deviation angles respectively from this analysis.

From the results shown in Figs. 2a and 2b, it is possible to estimate inertia effects. The term $u\partial u/\partial x$ has been determined at 10 km intervals from the information contained in the figures using a centered finite difference. Comparison was then made between the inertia term and the sloped-inversion pressure gradient force for the inversion strengths of Figs. 2a and 2b. The ratio of the inertia term to the sloped-inversion term over the idealized ice profile in (7) is shown in Fig. 3. Without question, inertia effects are negligible over the interior of the model continent. From this analysis, the restriction by Parish (1982) of limiting the streamline analysis over East Antarctica to the 2000 m contour seems conservative. If a ratio of 0.25 is taken as the threshold at which inertia effects become important, the equation system is a valid first approximation to the surface winds up to 75 km from the coast. The dashed line in Fig. 3 shows the ratio of inertia effects to the sloped-inversion force for the variable inversion strength specified above. As is clear from Fig. 3, the relative importance of the inertia term may be smaller than suggested from analyses using a constant inversion assumption.

Additional confirmation of the utility of the diagnostic equation system can be found in the work of Weller (1969). A series of field observations along the 62°E profile in East Antarctica from 600 km inland to 16 km offshore were made during 1961. The measurements of wind speed along the profile permit assessment of the magnitude of the inertia term. As can be verified from Fig. 1 in Weller (1969), the magnitude of the inertia term $u\partial u/\partial x$ averaged over the entire observational period and valid for a distance 75 km from the coast is about 2×10^{-4} m s^{-2}, generally an order of magnitude smaller than typical sloped-inversion pressure gradient forces. Only over the nearest 25 km to the coast does the inertia term reach a magnitude comparable to the sloped-inversion force. Weller (1969) concludes that the aforementioned steady state equation system successfully explains his field observations of wind speeds and deviation angles.

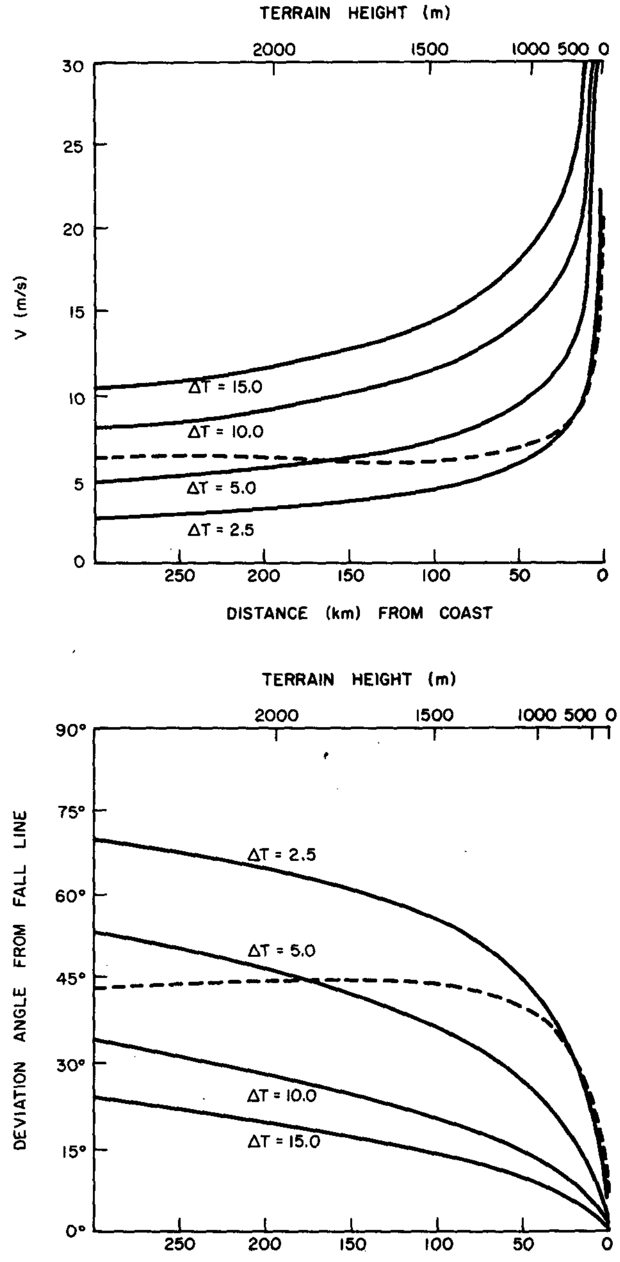

FIG. 2. Model results of (a) wind speed in m s^{-1} and (b) deviation angles of the surface wind from the fall line for various assumed values of inversion strength over the idealized Antarctic continent. Dashed lines in (a) and (b) indicate wind speeds and deviation angles for varying inversion strength as discussed in the text.

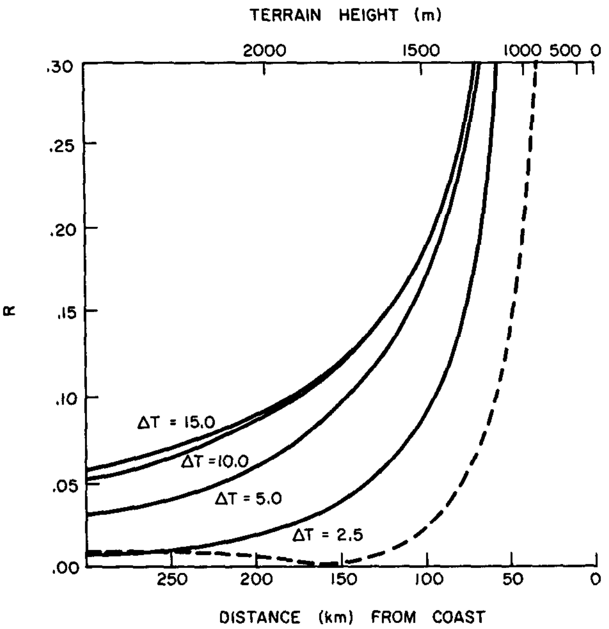

FIG. 3. Ratios (R) of the inertia term to the sloped-inversion pressure gradient force for various assumed values of inversion strength over the idealized Antarctic continent. Dashed line for same variable inversion strength as Fig. 2.

The conclusion to be reached from such analyses is that the simple diagnostic equation system outlined above yields qualitatively accurate simulations possibly to within 50 km of the coast. Over much of West Antarctica where coastal ice slopes are generally less than over East Antarctica, the equation system should permit diagnosis of the surface windfield to the coastline.

3. West Antarctic time-averaged near surface windfield

A major effort during the past decade has been the detailed mapping of the ice terrain of the Antarctic continent using primarily airborne radio echo soundings (Drewry, 1975; Jankowski and Drewry, 1981) but also constant density balloon altimetry and oversnow barometry. The terrain maps are essential to the understanding of near-surface drainage over Antarctica and have provided insight into anomalous katabatic-prone areas (Parish, 1981; Bromwich and Kurtz, 1984). The most recent mapping effort has focused on West Antarctica. According to Jankowski and Drewry (1981), terrain heights determined from the radio echo soundings have a mean error of 46.5 m. An ice topography map obtained by integrating the various height measuring techniques listed above can be found in Drewry (1983). This composite map represents a major improvement in the knowledge of the ice contours over West Antarctica. Height errors are considered significantly less than 50 m, perhaps near 30 m. This map serves as the basis for the analysis of the wintertime surface windfield to follow.

To generate drainage streamlines over the West Antarctic interior, it is necessary to digitize the ice height field. A total of 2000 grid points were taken off the Drewry (1983) map, the separation between grid points being 38 km which is adequate to resolve nearly all detail in the aforementioned map. Surface slopes are computed using a five-point-centered finite difference scheme. The strength and structure of the temperature inversion is also required to properly evaluate the terrain-induced accelerations. Previously, Parish (1982) used the work of Phillpot and Zillman (1970) to infer the inversion strength over East Antarctica. A clear relationship between terrain height and inversion strength can be seen in Fig. 12 in the work of Schwerdtfeger (1970a). Results for West Antarctica are less certain, although average inversion strengths are unquestionably less than found over the high plateau of East Antarctica. The aforementioned Phillpot and Zillman map shows average inversion strength to range from 5°C near the coast to about 15°C over the interior and along Weddell Sea coast. The differences in inversion strength between East and West Antarctica can be attributed in part to slope differences. Slopes over the interior of West Antarctica are considerably steeper than the high plateau regions of East Antarctica. The stronger sloped-inversion forcing and resulting mixing processes possibly limit the strength of the inversion.

Of prime importance in the proper evaluation of the sloped-inversion pressure gradient force at the surface is the structure of the inversion. The integrated temperature deficit from ambient conditions over the entire inversion depth is the important parameter needed to correctly diagnose the terrain-induced accelerations. Budd et al. (1966) have summarized results from 32 rapid-run radio soundings at Byrd station taken during 1962–63, showing that the wintertime temperature structure differs markedly from the exponential-shaped profiles prevalent over East Antarctica. Inversion strengths generally are less than 10 K and the profile structures are generally of a well-mixed type (e.g., see Fig. 15 in Budd et al., 1966). Schwerdtfeger (1970a) notes that Byrd station has a mean wintertime (April–September) inversion strength of 9.5 K from approximately 1000 soundings taken at 0400 LT and 9.2 K from a similar number of soundings at 1600 LT. The 14-year resultant wind magnitude at Byrd during winter is about 8.9 m s^{-1}. The moderately strong wind speeds and relatively weak inversion strengths (compared to East Antarctic interior stations) suggest that the inversion structure is relatively well-mixed at Byrd and probably over most of the slopes of interior West Antarctica.

Wintertime inversion strengths over West Antarctica are assumed related to terrain elevation similar to that in Parish (1982). Rough estimates can be obtained from the map in Schwerdtfeger (1970a) as well as from the Byrd station data. The assumed functional form of inversion strength can be expressed by,

$$\Delta T = (z - 1200.0\ \mathrm{m})/1000.0\ \mathrm{m} + 10.0.$$

This expression is only qualitatively accurate. The details of the average inversion strengths over the continent are not known. Using the terrain slopes from the Drewry (1983) map of West Antarctica and assumptions made above regarding the shape and strength of the wintertime inversion, we note that the diagnostic equation system can be used to infer the time-averaged inversion windfield. Computations were made for each grid point covering the 40 × 50 grid domain. As in the Parish (1982) East Antarctic simulation, wind speeds are quite uniform over West Antarctica, reflecting local slope gradients. The model wind for the position corresponding to Byrd station is 8.8 m s^{-1} from approximately 015°. These numbers compare very favorably to actual wintertime resultant winds given in Schwerdtfeger (1970a). Of significance is the streamline pattern of the inversion wind drainage currents. The streamline analysis of the time-average inversion windfield is shown in Fig. 4. The analysis is extended nearly to the coast since terminal slopes are considerably less than over East Antarctica and the wind inertia effects are probably small. The West Antarctic interior height field is considerably more complex than that found in East Antarctica and the streamline analysis in Fig. 4 shows the drainage pattern to be quite irregular. Clearly revealed are several zones where the drainage currents converge as the flow nears the coastline. The importance of cold air confluence in the interior of Antarctica on coastal katabatic flow has been discussed in Parish (1981, 1982) as well as in Bromwich and Kurtz (1984). Implications of the West Antarctic flow regime will be discussed in Section 5.

The inversion structure and strength used in the equation system to arrive at inversion wind estimates are the most uncertain parameters. In order to check the sensitivity of the analysis in Fig. 4, numerous tests were conducted in which the inversion structure and strength were allowed to vary. The inversion winds were again calculated at each grid point and a streamline analysis was made similar to Fig. 4. An example is illustrated in Fig. 5, in which the inversion strength has been reduced by a factor of 2 compared to Fig. 4. The inversion wind speeds show a decrease in response to the weaker temperature inversions. It is felt that the

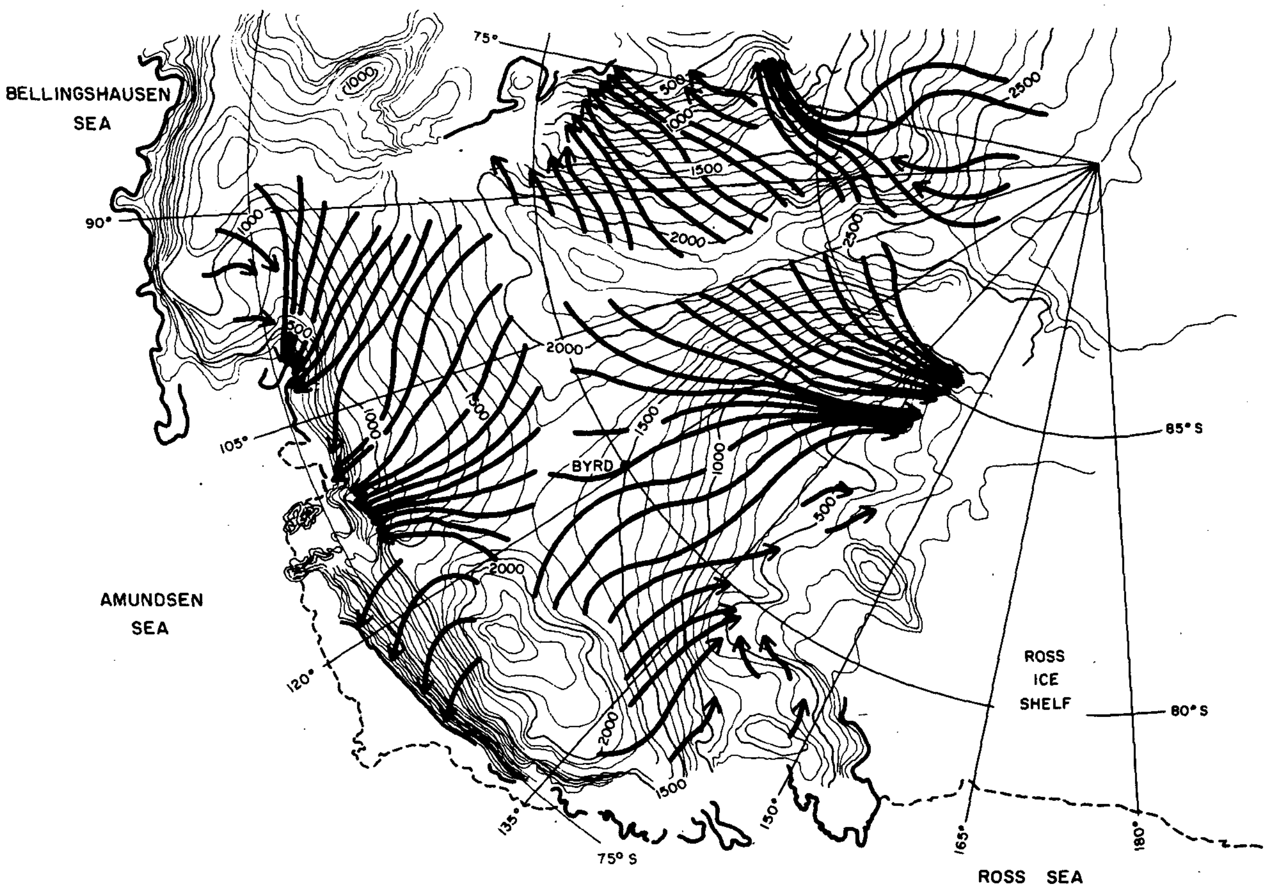

FIG. 4. Time-averaged winter streamline pattern of surface airflow over West Antarctica based on model calculations discussed in the text.

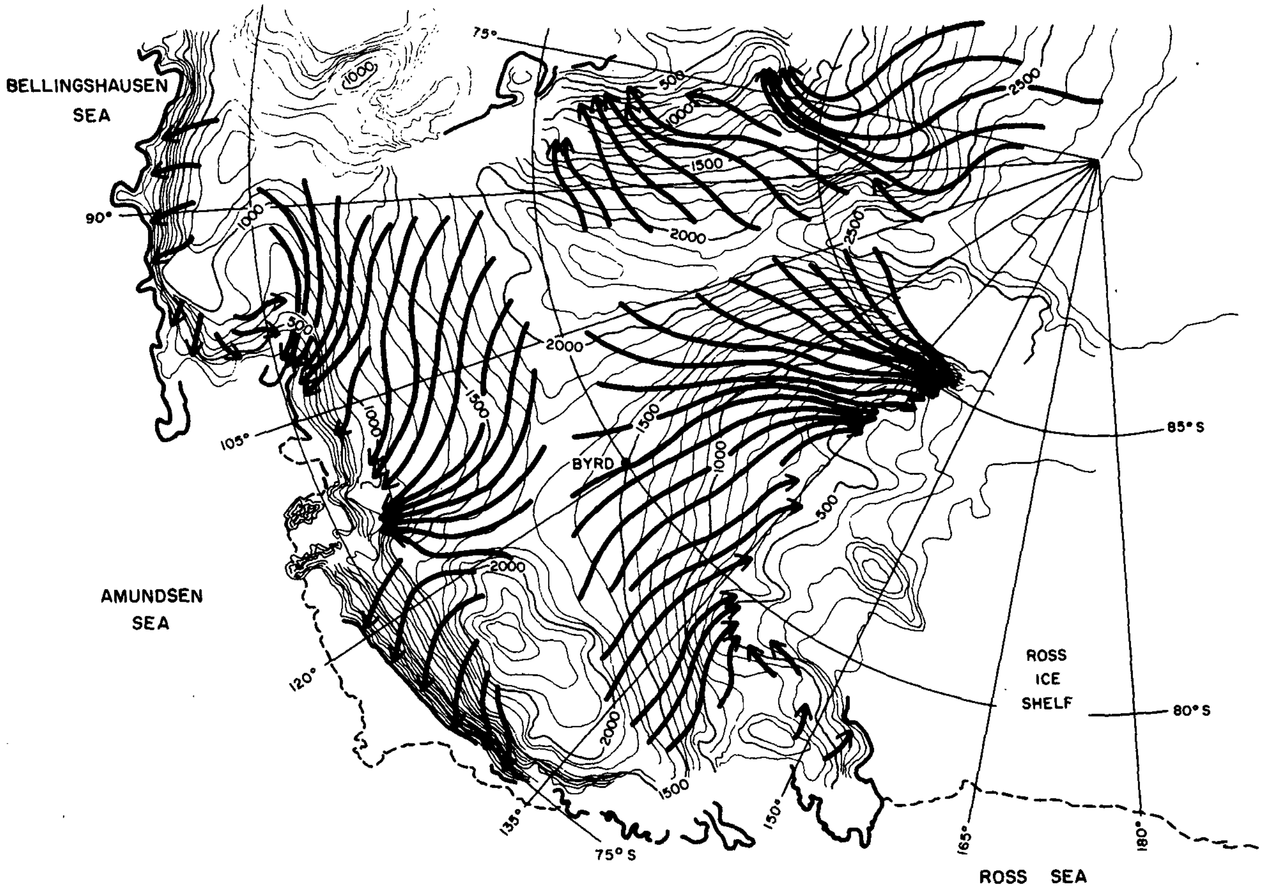

FIG. 5. As in Fig. 4 except assumed inversion strengths are reduced by a factor of 2.

assumed values represent a lower limit to the expected inversion strengths. For example, at Byrd station an inversion strength of about 7 K is estimated and the wind speed diagnosed from the equation system is 4.1 m s^{-1} from approximately 005°. These values are close to the resultant wind vector over the summer months are shown in Schwerdtfeger (1970a). The assumed inversion strength is also less than the mean wintertime values reported earlier. However, the streamline pattern in Fig. 5 still shows the same large scale flow characteristics as Fig. 4. Close examination reveals the streamlines in Fig. 5 are directed in a more contour-parallel direction, yet the confluence zones are still clearly defined and in approximately the same position as in Fig. 4. Results from other model runs show qualitatively similar features. One result of this sensitivity study is that the large scale drainage pattern seems somewhat insensitive to the precise terrain-induced forcing. There is some evidence to suggest this result may be realistic. Resultant wind directions over the summer months for East Antarctic interior stations generally vary from corresponding values in winter months by about 20° despite the marked differences in the magnitude of the sloped-inversion pressure gradient force. It can be concluded that the large scale surface flow representation in Fig. 4 is probably a good qualitative estimate of the time-averaged wintertime inversion wind pattern over the surface of West Antarctica.

4. Verification

The relative scarcity of conventional surface weather observations over the West Antarctic ice sheet dictates that the simulated airflow must be validated primarily by indirect evidence. The main data base consists of sastrugi orientations observed during oversnow traverses operating out of Byrd station soon after the International Geophysical Year (1957–58). Because most observations of these wind generated features are taken during the summer half year, a key assumption is that persistent unidirectional winds blow year round; this is demonstrated by the high directional constancy values observed at Byrd station during all months (Schwerdtfeger, 1970a). Bromwich and Kurtz (1984) show that sastrugi directions on the East Antarctic plateau agree closely with Parish's (1982) simulation. All sastrugi observations available in the literature

(Brecher, 1964; Shimizu, 1964) have been plotted on Fig. 6 for comparison with the derived streamlines. In addition, a subset of the large number of sastrugi directions which were recorded by W. E. Long during the Horlick Mountains Traverse 1958–59 and which are archived at the Institute of Polar Studies has been utilized. These last data are averages over 11.2 km increments of primary sastrugi orientations observed every 5.6 km. Figure 6 shows that sastrugi data provide strong confirmation for the streamline confluence upslope from the Siple Coast; both the observations and model output depict the systematic change from NNE airflow at Byrd station to easterly drainage along the Transantarctic Mountains.

Additional confirmation of the Siple Coast confluence is provided by surface wind measurements taken at temporary camps occupied as part of the Siple Coast Glaciology Project during the 1984/85 austral summer. One camp (Upstream B) was also in operation during the previous summer. Observations using hand-held instruments were taken irregularly at least three times each day. Vector averages for each day were calculated from all data, and these in turn were composited over the period of record to give the results in Table 1. To partially evaluate the impact of varying observation intervals, resultant winds at the Byrd AWS were derived for all these periods; Figs. 4 and 5 show that this site is far upslope of the temporary camps but part of the same drainage system. The Byrd results suggest that the vector average speeds and directional constancies (and therefore scalar average wind speeds) for the temporary camp locations are representative, but that the resultant wind directions are unreliable. Table 1 demonstrates that the directional constancy and wind speed in the simulated confluence zone (South camp) are much higher than those outside it (North and Upstream B camps). High directional constancies and enhanced wind speeds have been observed downstream of two East Antarctic confluence zones: at Cape Denison (Parish, 1982) and in Terra Nova Bay (Bromwich, 1985).

It appears from Fig. 6 that the simulation is invalid within a few hundred meters downslope to the east of the ice divide near 84°S, 95°W. The consistency in

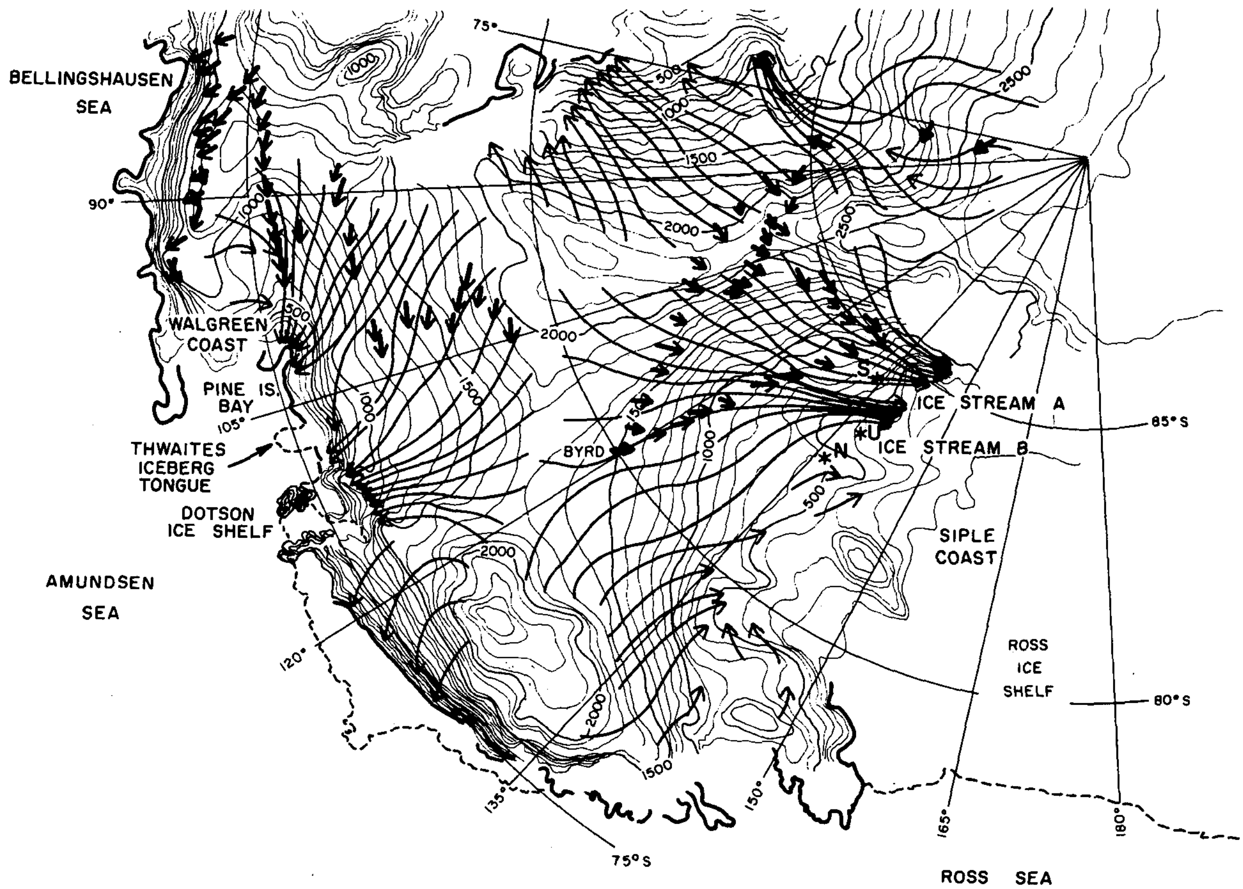

FIG. 6. Comparison of surface airflow simulation in Fig. 4 (thin lines) with observed sastrugi orientations (short, bold arrows). The open headed arrows to the south and southwest of Byrd station are taken from observations of W. E. Long; those to the northeast of Byrd are from Shimizu (1964). The closed-headed arrows are due to Brecher (1964). The asterisks labeled N, U and S represent North, Upstream B and South camps, respectively.

TABLE 1. Surface wind statistics for sites in and around the Siple Coast confluence zone.

Period of record at temporary station	Temporary station: Resultant wind at 1.5 m	Temporary station: Directional constancy	Byrd* AWS for period of record: Resultant wind at 3 m	Byrd* AWS: Directional constancy	Speed ratio (temporary station ÷ Byrd)
	North Camp				
10 Dec 84–8 Jan 85	81° 1.7 m s^{-1}	0.55	55° 4.6 m s^{-1}	0.82	0.54
	Upstream B Camp				
10 Nov 83–25 Jan 84	69° 2.3 m s^{-1}	0.77	41° 4.1 m s^{-1}	0.73	0.53
1 Dec 84–18 Jan 85	95° 2.5 m s^{-1}	0.78	36° 4.1 m s^{-1}	0.77	0.61
	South Camp				
21 Dec 84–7 Jan 85	87° 6.4 m s^{-1}	0.97	23° 4.5 m s^{-1}	0.86	1.25 1.38**

* Climatological 10 m resultant wind for Byrd station for December and January combined is from 003° at 4.8 m s^{-1} with a directional constancy of 0.78 (Schwerdtfeger, 1970a).

** Speed ratio calculated for 12/11/84–1/7/85 by using a composited speed record from South Camp; visually estimated values were available from 11–20 December and measured speeds from 21 December to 7 January.

this area of the Long and Brecher sastrugi observations which were collected during separate summers indicates that this disagreement is a persistent feature, and suggests that there may be a contribution from East Antarctica to the Siple Coast confluence. This interpretation was adopted by Mather (1969) for his broadscale streamline analysis. The 1970 American Geographical Society map of Antarctica suggests that the topography in this area is more complicated than that resolved by Drewry's (1983) synthesis, upon which the present modeling results depend. However, prevailing upslope winds have been observed just to the east of an ice divide well inland from Syowa station (Inoue et al., 1983). Such flows may result from inertia effects on drainage winds from higher elevations; the inertia terms have been omitted from the model's equations of motion. For ice divide areas where the synoptic forcing is strong (i.e., around 75°S, 83°W) frictionally deflected geostrophic flow may generate the sastrugi.

Sastrugi directions in Fig. 6 are consistent with the pronounced confluence regions into the Amundsen Sea but are insufficient to completely confirm them. Additional supporting evidence is available however. Streten (1973) evaluated low resolution (~54 km) 5-day hemispheric minimum brightness mosaics and noted the presence of large polynyas (areas of open water surrounded by ice) on either side of the Thwaites Iceberg Tongue. He suggested that katabatic winds may play a role in their formation. A more detailed examination of sea ice conditions in the Amundsen Sea was conducted by Mitchell and Potocsky (1974). They constructed weekly sea ice charts from comparatively high resolution (~6 km) visible satellite imagery over the period from October to February for the years 1969–74. Most importantly, they noted when no analysis was possible because clouds obscured the surface. On the first cloud-free chart of each austral summer an area of reduced ice concentration was analyzed along and to the north of the Dotson Ice Shelf, i.e., immediately offshore from the most pronounced confluence into the Amundsen Sea; the polynya persisted through each summer. Monthly mean sea-ice concentration maps constructed by Zwally et al., (1983) from passive microwave observations also show this spring and summer polynya as a prominent feature.

It is suggested that this persistent spring polynya is caused by pronounced katabatic winds which sometimes cross the ~130 km from the foot of the terrain slope to the edge of the Dotson Ice Shelf. Bromwich and Kurtz (1984) and Knapp (1972) demonstrate that polynyas form on the lee side of fixed obstacles when sea ice is blown away by strong winds. In general, katabatic winds either completely dissipate within a few kilometers beyond the end of the terrain slope (Schwerdtfeger, 1970a) or would be substantially slowed by friction over a horizontal distance of 130 km (Bromwich and Kurtz, 1984); it thus appears that the assistance of marked pressure gradients associated with passing cyclones is required to maintain or accelerate the strong katabatic winds across the Dotson Ice Shelf. This airflow would also be channeled by the steep headlands on either side of the shelf. Presumably, ice does not reform in the interval between storms because of generally rising air temperatures and absorption of large quantities of solar radiation by the open water (compare Andreas and Makshtas, 1985). A similar spring and summer polynya occurs offshore from the Cape Denison confluence zone (Zwally et al., 1983) even though the katabatic wind is *usually* observed to dissipate close to the coastal slopes (Ball, 1957).

The Mitchell and Potocsky analyses showed spring and summertime open water immediately adjacent to the north–south part of the Walgreen Coast, slightly to the east of the polynya location noted by Streten (1973). The frequent absence of open water in Pine Island Bay means that these analyses cannot be used to validate the confluence simulated in that area. It appears as though the open water west of the Walgreen Coast is generated almost entirely by strong easterly winds generated by passing cyclones (Knapp, 1972).

5. Conclusions and implications

Surface winds over the Antarctic continent are controlled by topography. The strong radiational cooling of air adjacent to the sloping ice terrain results in the establishment of a sloped-inversion pressure gradient force which is the primary driving mechanism for all Antarctic slope flows. As a result, near-surface winds are characterized by extremely high directional constancy values, generally in excess of 0.80. The strong influence of the ice topography and steady state nature of the surface winds permit representative and very simple diagnosis of the inversion windfield provided the detailed ice topography and thermodynamic structure of the lower atmosphere are known. By using the most recent ice terrain information of Antarctica based on results of airborne radio echo soundings and climatologically derived estimates of the temperature inversion strength and structure, a picture of the time-averaged near-surface winter inversion windfield is obtained.

The most prominent features revealed in the West Antarctic near-surface streamline map of Fig. 4 are the major confluence zones where cold air drainage currents from a broad interior section converge through a constricted coastal region. Such features are considered to be major factors in shaping the character of coastal katabatic winds. Lettau and Schwerdtfeger (1967) point out that a serious limitation to the strength and persistence of coastal katabatic flow is the availability of a supply of radiatively produced, negatively buoyant air upslope in the interior of the continent. Parish (1981, 1984) has shown katabatic winds to be particularly sensitive to the upstream inversion windfield. A convergent pattern of inversion winds results in an enhanced supply of cold air which enables a more intense and persistent katabatic stream. Evidence presented earlier suggests a local strengthening of katabatic winds along two of the inversion wind confluence zones. Complete confirmation of the relationship between simulated confluence zones and enhanced katabatic winds awaits further observational evidence. It is unlikely, however, that a katabatic regime similar to that reported at either Cape Denison (Parish, 1981) or Terra Nova Bay (Bromwich and Kurtz, 1982, 1984) exists in West Antarctica. The most striking confluence zone is found near the Siple Coast, along the eastern edge of the Ross Ice Shelf. The size of the drainage area and degree of streamline confluence are representative of the simulated airflow features in East Antarctica (Parish, 1982). However, the terrain slopes along the Siple Coast are considerably more gentle than corresponding ice slopes in East Antarctica and weaker katabatic winds are to be expected.

Even so, the Siple Coast confluence will almost continually inject large volumes of cold air onto the Ross Ice Shelf in a direction roughly parallel to the Transantarctic Mountains. This cold air should play an important role in the boundary layer regime of the Ross Ice Shelf and, in particular, may be a major mass source for the frequent southerly winds observed year round in the northwestern corner of the shelf near Ross Island (Schwerdtfeger, 1984).

The Siple Coast confluence is also relevant to glaciological investigations of Ice Streams A and B. Blowing and drifting snow were frequently observed at South Camp. Therefore, the enhanced confluence winds will probably cause a substantial redistribution of precipitated snow. This important effect should be carefully evaluated for studies of this area's accumulation distribution and firn stratigraphy.

Carleton (1981) examined winter (June to September) thermal infrared satellite images for 1973–77 and demonstrated the existence of a band of high-latitude cyclogenesis (the Winter Antarctic Front) with maxima north-northwest of the Ross Sea and to the north of the Bellingshausen Sea. These winter maxima reflect frequent formation of "inverted-comma" type cyclones associated with cold air outbreaks from the Antarctic continent, and are 30–35 degrees of longitude to the east of the zones of enhanced katabatic outflow near Cape Denison (Parish, 1981) and into the Amundsen Sea. It is suggested that enhanced katabatic drainage may play a role in these developments by generating (during undisturbed periods) large coastal pools of cold boundary layer air. When this cold air is advected northward over regions with marked sea surface temperature gradients, cyclogenesis could occur by intense diabatic heating in combination with CISK and/or moist baroclinicity; these mechanisms are inferred to be the key ingredients for polar low formation in the Northern Hemisphere (Sardie and Warner, 1983; Forbes and Lottes, 1985). Lyons (1983) notes that "intense Antarctic" depressions affect the southern tip of South America when upper level steering winds are favorable. The strongest storms move from the south-southwest with speeds in excess of 18 m s^{-1}. Assuming that many of these lows originate in the Amundsen Sea from the processes described here and that 18 m s^{-1} is a representative year-round speed, an incipient eastward-moving disturbance would take less than 1 day to evolve into an "inverted-comma" type cyclone resolvable on the (comparatively low resolution) satellite imagery used by Carleton (1981). This inferred development time scale is generally consistent with the North Atlantic results of Forbes and Lottes (1985).

The pattern of inversion winds, revealed in Fig. 4 for West Antarctica as well as in Parish (1982) for East Antarctica, shows a high degree of irregularity. Near-surface cold air drainage currents do not display a uniform radial pattern about the high plateau regions but rather are strongly concentrated into several zones. This view differs from the horizontally uniform conditions assumed by Radok (1973) in his estimate of energetics of katabatic winds. It is possible that the majority of the cold air transport from katabatic winds takes place along these convergent channels. This is substantiated in part by results of numerical simulations of katabatic winds presented in Parish (1984). The cold air depth, as well as the katabatic wind speed, is significantly enhanced along the axis of the confluence zone. Thus, the cold air transport is extremely sensitive to the confluent nature of the surface drainage pattern.

As noted by Radok (1973), even a rough assessment of the energetics of katabatic winds about the Antarctic continent is difficult owing to the lack of simultaneous observations in the katabatic wind layer. However, it is possible that the katabatic regime represents an important component in the Antarctic energy budget and may even play a significant role in the entire Southern Hemisphere meridional heat transport. The highly irregular katabatic drainage pattern implies a horizontally inhomogeneous heat transport, emphasizing the importance of cold air confluence zones represented in the simulated time-average surface airflow patterns over East and West Antarctica. It seems clear that the influence of simulated confluence channels must be considered to arrive at correct estimates of the fluxes of sensible and latent heat across the coastline.

One disturbing result which underscores the inadequacy of the current understanding of the role of Antarctica on Southern Hemisphere climate is the poor performance of atmospheric general circulation models (AGCMs) in simulating the position and intensity of circumpolar lows in the Southern Hemisphere as well as surface temperature, precipitation and pressure over Antarctica. In a summary article by Schlesinger (1984) focusing on the performance of AGCMs in simulating the Antarctic climate, surface temperatures in the interior of Antarctica as predicted by the models are typically between 10–20 K warmer than observed; this statement is based upon model comparisons with the Taljaard et al. (1969) climatology. The high quality and continuing validity of this synthesis can readily be demonstrated by comparing grid point values with the observed air temperatures given in Schwerdtfeger (1970a) for Byrd, South Pole, Vostok and Plateau stations, and by noting the weak warming trend between 1957 and 1982 (Raper et al., 1984). Herman and Johnson (1980) attribute large surface temperature errors in the Goddard Laboratory for Atmospheric Science (GLAS I) model to problems in treating the surface energy balance over the high plateau. They note that more realistic representations of ice-ocean-atmosphere interactions may be required to remedy model deficiencies. In most AGCMs, the Antarctic topography is smoothed considerably, resulting in a decrease of the height of the high plateau regions and especially of the steepness of the near-coastal terrain. In addition, the relatively coarse horizontal grid spacing (for example, 4° lat by 5° long for the GLAS I model) prevents accurate model specification of Antarctic terrain irregularities. Furthermore, the small number of vertical layers (generally less than 10) limits resolution of shallow drainage features. Thus, even AGCMs with relatively detailed radiational parameterization schemes tend to significantly underestimate the katabatic wind influence. This is especially important in simulations that seek to ascertain the impact of changes in atmospheric carbon dioxide content upon the West Antarctic surface energy balance; the wind and temperature regimes in the shallow near-surface layer are strongly coupled and need be treated as such in modeling calculations. Obviously AGCMs are constrained by speed and memory considerations, but some parameterized methods of incorporating katabatic winds and, in particular, the confluence zones shown in the East and West Antarctic simulations would seem appropriate in light of the difficulty in current AGCM simulations of the Southern Hemisphere and Antarctica. Such studies may also provide insight as to the importance of katabatic flows on energetics of the Antarctic atmosphere.

Acknowledgments. Ian Whillans, Henry Brecher, George Doumani and Walt Seelig helped us acquire validation data for the airflow simulation. Jeff DeFreest, Andrea Donnellan, Joe Kostecka, Mike Strobel and Patricia Vornberger collected the observations at North and South camps as part of NSF Grant DPP-8117235A02; Upstream B data were taken by ITT Antarctic Services Incorporated personnel. Collection and distribution of Byrd AWS data were supported by NSF Grant DPP-8306265 to Charles R. Stearns. All this assistance and input are gratefully acknowledged. This research was funded by NSF Grants DPP-8115976 to T. R. Parish and DPP-8314613 to D. H. Bromwich.

REFERENCES

Andreas, E. L., and A. P. Makshtas, 1985: Energy exchange over Antarctic sea ice in the spring. *J. Geophys. Res.*, **90**, 7199–7212.

Ball, F. K., 1957: The katabatic winds of Adelie Land and King George V Land. *Tellus*, **9**, 201–208.

——, 1960: Winds on the ice slopes of Antarctica. *Antarctic Meteorology, Proc. of the Symposium,* Melbourne, 1959, Pergamon, 9–16.

Brecher, H. H., 1964: Glaciological observations on the Byrd Station–South Pole traverse, 1960–61. *J. Glaciol.*, **5**, 339–343.

Bromwich, D. H., 1984: Precipitation regime of the West Antarctic ice sheet. *Environment of West Antarctica: Potential CO_2-Induced Changes,* National Academy Press, Washington, DC, 107–115. [Polar Research Board, 2101 Constitution Avenue, N.W., Washington, DC. 20418.]

——, 1985: Katabatic wind interaction with Inexpressible Island, Terra Nova Bay. *Antarctic. J. U.S.*, in press.

——, and D. D. Kurtz, 1982: Experiences of Scott's Northern Party: Evidence for a relationship between winter katabatic winds and the Terra Nova Bay polynya. *Polar Record,* **21**, 137–146.

——, and ——, 1984: Katabatic wind forcing of the Terra Nova Bay polynya. *J. Geophys. Res.*, **89**, 3561–3572.

Budd, W. F., W. R. J. Dingle and U. Radok, 1966: The Byrd snowdrift project: outline and basic results. *Studies in Antarctic Meteorology, Antarctic Research Series,* Vol. 9, Amer. Geophys. Union, 71–134. [American Geophysical Union, 2000 Florida Avenue, N.W., Washington, D.C., 20009.]

Carleton, A. M., 1981: Ice-ocean-atmosphere interactions at high southern latitudes in winter from satellite observations. *Austr. Meteor. Mag.*, **29**, 183–195.

Cerni, T. A., and T. R. Parish, 1984: A radiative model of the stable nocturnal boundary layer with application to the polar night. *J. Climate Appl. Meteor.*, **23**, 1563–1572.

Drewry, D. J., 1975: Radio echo sounding map of Antarctica. *Polar Record*, **17**, 359–374.

——, 1983: The surface of the Antarctic ice sheet. Sheet 2 of *Antarctica: Glaciological and Geophysical Folio*, D. J. Drewry, Ed., Scott Polar Research Institute, Cambridge. [Scott Polar Research Institute, University of Cambridge, Lensfield Road, Cambridge CB2 1ER, UK.]

Forbes, G. S., and W. D. Lottes, 1985: Classification of mesoscale vortices in polar airstreams and the influence of the large-scale environment on their evolutions. *Tellus*, **37A**, 132–155.

Herman, G. F., and W. T. Johnson, 1980: Arctic and Antarctic climatology of a GLAS general circulation model. *Mon. Wea. Rev.*, **108**, 1974–1991.

Inoue, J., H. Nishimura and K. Satow, 1983: The climate of the interior of Mizuho Plateau. *Proc. Fifth Symp. Polar Meteor. Glaciol., Memoirs of National Institute of Polar Research*, Special issue No. 29, Tokyo, 24–36. [National Institute of Polar Research, 9–10, Kaga 1-chome, Itabashi-ku, Tokyo 173, Japan.]

Jankowski, E. J., and D. J. Drewry, 1981: The structure of West Antarctica from geophysical studies. *Nature*, **291**, 17–21.

Knapp, W. W., 1972: Satellite observations of large polynyas in polar waters. *Sea Ice*, T. Karlsson Ed., National Research Council, Reykjavik, Iceland, 201–212. [National Research Council of Iceland, Laugaveg 13, Reykjavik, Iceland.]

Kodama, Y., and G. Wendler, 1986: The wind and temperature regime along the slope of Adelie Land, Antarctica. *J. Geophys. Res.*, in press.

Lettau, H. H., and W. Schwerdtfeger, 1967: Dynamics of the surface-wind regime over the interior of Antarctica. *Antarct. J. U.S.*, **2**, 155–158.

Lyons, S. W., 1983: Characteristics of intense Antarctic depressions. *Preprints, First Int. Conf. Southern Hemisphere Meteorology.* Sao Jose Dos Campos, Amer. Meteor. Soc., 238–240.

Mather, K. B., 1969: The pattern of surface wind flow in Antarctica. *Pure Appl. Geophys.*, **75**, 332–354.

——, and G. S. Miller, 1966: Wind drainage off the high plateau of Eastern Antarctica. *Nature*, **209**, 281–284.

——, and ——, 1967: Notes on topographic factors affecting the surface wind in Antarctica, with special reference to katabatic winds, and bibliography. Geophys. Inst. Rep. UAG R-189, University of Alaska, 125 pp. [Geophysical Institute, University of Alaska, Fairbanks, Alaska 99701.]

Mitchell, P. A., and G. J. Potocsky, 1974: Ice conditions in the Pine Island Bay area, western Antarctica, as derived from satellite imagery (October 1969–February 1974). U.S. Naval Oceanographic Office, Tech. Note No. 6150-30-74, Washington, D.C. [U.S. Naval Oceanographic Office, Washington, D.C. 20373.]

Parish, T. R., 1981: The katabatic winds of Cape Denison and Port Martin. *Polar Record*, **20**, 525–532.

——, 1982: Surface airflow over East Antarctica. *Mon. Wea. Rev.*, **110**, 84–90.

——, 1984: A numerical study of strong katabatic winds over Antarctica. *Mon. Wea. Rev.*, **112**, 545–554.

Phillpot, H. R., and J. W. Zillman, 1970: The surface temperature inversion over the Antarctic continent. *J. Geophys. Res.*, **75**, 4161–4169.

Radok, U., 1973: On the energetics of surface winds over the Antarctic ice cap. *Energy fluxes over polar surfaces*, WMO Tech. Note No. 129, Geneva, Switzerland, pp. 69–100. [World Meteorological Organization, Case postale No. 5, CH-1211, Geneva 20, Switzerland.]

Raper, S. C. B., T. M. L. Wigley, P. R. Mayes, P. D. Jones and M. J. Salinger, 1984: Variations in surface air temperatures. Part 3. The Antarctic, 1957–82. *Mon. Wea. Rev.*, **112**, 1341–1353.

Sardie, J. M., and T. T. Warner, 1983: On the mechanism for the development of polar lows. *J. Atmos. Sci.*, **40**, 869–881.

Schlesinger, M. E., 1984: Atmospheric general circulation model simulations of the modern Antarctic climate. *Environment of West Antarctica: Potential CO_2-Induced Changes*, National Academy Press, Washington, D.C., 155–196. [Polar Research Board, 2101 Constitution Avenue, N.W., Washington, D.C. 20418.]

Schwerdtfeger, W., 1970a: *The Climate of Antarctica*, Vol. 14, S. Orvig., Ed., *World Survey of Climatology*, H. E. Landsberg, Ed., Elsevier, 253–355.

——, 1970b: Du temperaturinversion uber dem antarktischen plateau und die struktur ihres windfeldes. *Meteor. Rundsch.*, **23**, 164–171.

——, 1984: *Weather and Climate of the Antarctic*, Elsevier, 261 pp.

Shimizu, H., 1964: Glaciological studies in West Antarctica, 1960–1962. *Antarctic Snow and Ice Studies, Antarctic Research Series*, Vol. 2, Amer. Geophys. Union, 37–64. [American Geophysical Union, 2000 Florida Avenue, N.W., Washington, D.C. 20009.]

Streten, N. A., 1968: Some characteristics of strong wind periods in coastal East Antarctica. *J. Appl. Meteor.*, **7**, 46–52.

——, 1973: Satellite observations of the summer decay of the Antarctic sea-ice. *Arch. Meteor. Geophys. Bioklim.*, **A22**, 119–132.

Taljaard, J. J., H. van Loon, H. L. Crutcher and R. L. Jenne, 1969: *Climate of the Upper Air: Southern Hemisphere*, Vol. 1. Temperature, dew points and heights at selected pressure levels. NAVAIR-50-1C-55, Chief Naval Operations, Washington, D.C., 135 pp. [Commander, Naval Weather Service Command, Washington Navy Yard, Building 200, Washington, D.C. 20390.]

Weller, G. E., 1969: A meridional surface wind speed profile in MacRobertson Land, Antarctica. *Pure Appl. Geophys.*, **77**, 193–200.

Wendler, G., Y. Kodama and A. Poggi, 1982: The climate of Dome C. *Antarct. J. U.S.*, **17**, 201–203.

Zwally, H. J., J. C. Comiso, C. L. Parkinson, W. J. Campbell, F. D. Carsey and P. Gloersen, 1983: *Antarctic sea ice, 1973–1976: Satellite Passive-Microwave Observations.* NASA, SP-459, National Aeronautics and Space Administration, Goddard Space Flight Center, Greenbelt, MD., 206 pp. [U.S. Government Printing Office, Washington, D.C. 20402.]